Available online at www.sciencedirect.com
ScienceDirect
Applied Clay Science 42 (2008) 224–231
Applied CLAY Science
www.elsevier.com/locate/clay

Structure of cetyltrimethylammonium intercalated hydrobiotite

Runliang Zhu, Lizhong Zhu *, Jianxi Zhu, Liheng Xu

Department of Environmental Science, Zhejiang University, Hangzhou 310028, China

Received 28 February 2007; received in revised form 4 December 2007; accepted 7 December 2007
Available online 28 December 2007

Abstract

Surfactant–clay mineral complexes obtained by intercalating cationic surfactants have attracted much scientific and industrial attention because of the wide applications in many fields. In this work we selected hydrobiotite to synthesize novel surfactant–clay mineral complexes with unique structures. Various amounts of cetyltrimethylammonium cations were intercalated into hydrobiotite and montmorillonite (for comparison). The structure of the surfactant–clay mineral complexes was characterized by X-ray diffraction, Fourier transform infrared spectroscopy and thermogravity analysis. Whereas the interlayer spaces of the montmorillonite were simultaneously intercalated and expanded by the surfactant cations, the hydrobiotite could only be intercalated and expanded layer by layer. Conformations of the intercalated surfactant cations on montmorillonite developed gradually from "liquidlike" to "solidlike" with increasing surfactant loading, whereas the intercalated surfactants on hydrobiotite adopted "solidlike" conformation even at very low surfactant loading stages. Both Coulombic interaction between the surfactant head groups and the clay mineral charge sites and van der Waals interaction between surfactant alkyl chains played important role for the intercalation of hydrobiotite. The unique structures of the surfactant–hydrobiotite may render them special properties and utilities.

Keywords: Montmorillonite; Hydrobiotite; Surfactants

1. Introduction

Surfactant intercalated clay minerals have attracted great interest owing to their academic and industrial importance. They have found wide applications in rheological controlling of paints and greases (Murray, 2000; Chtourou et al., 2006), removal of organic contaminants (Zhu et al., 1998; Witthuhn et al., 2005), and as precursors in the synthesis of polymer intercalated nanocomposites (LeBaron et al., 1999; Lin et al., 2001). The confined surfactant nanophases are also used as models for investigating the partition of organic compounds into soil organic matter (Zhu et al., 2003a,b), and the interaction between biomolecules and lipid bilayers (Lagaly, 1976; Venkatatraman and Vasudevan, 2003).

Properties of the surfactant–clay mineral complexes are governed by their structures. For example, the microenvironment of the interlayer spaces determines their affinity toward organic compounds and polymers, which further determines the sorption capacities of the complexes toward organic contaminants (Chen et al., 2005; Zhu et al., 2007) and the exfoliation of the particles by polymers (LeBaron et al., 1999; Lee and Kim, 2002). To meet the special requirements from different fields, it is necessary to synthesize diverse complexes with quite different structures and properties. A large number of researches showed that the factors as surfactant structure, surfactant loading amount and clay mineral charge characteristics can have great influence on the structures of the complexes (Vaia et al., 1994; Osman et al., 2004; Osman 2006; Lagaly and Dekany, 2005; He et al., 2005, 2006; Heinz et al., 2006). Thereby, it is feasible to obtain complexes with designed structures and properties of the complexes by regulating these factors.

Montmorillonite is the most widely used clay mineral for synthesizing surfactant–clay mineral complexes (Xi et al., 2005a,b; Zhu et al., 2003a,b). Many previous investigations have shown that the intercalated surfactant cations can adopt diverse conformations (e.g., from "liquidlike" to "solidlike")

* Corresponding author. Tel.: +86 571 88273733; fax: +86 571 88273450.
E-mail address: zlz@zju.edu.cn (L. Zhu).

0169-1317/$ - see front matter © 2008 Elsevier B.V. All rights reserved.
doi:10.1016/j.clay.2007.12.004

within montmorillonite interlayer spaces as surfactant loading amount and molecular volume increased (Bergaya et al., 2006; Vaia et al., 1994; Osman et al., 2004; Zhu et al., 2005). However, because of the low layer charge density (0.25–0.45 eq/mol), it is hard to obtain very high surfactant packing density for the surfactant–montmorillonite complexes, especially in the low surfactant loading range and with small surfactant cations (Vaia et al., 1994; Lagaly and Dekany, 2005). Some investigations also used vermiculite with higher layer charge density (0.5–0.8 eq/mol), for synthesizing surfactant–clay mineral complexes (Yariv, 2002; Osman, 2006). However, the surfactant–vermiculite complexes have different structures comparing with surfactant–montmorillonite, e.g., larger basal spacings and higher surfactant packing density (Yariv, 2002; Lagaly and Dekany, 2005; Osman, 2006). Osman (2006) believed that the surfactant–vermiculite complexes will render the clay-polymer nanocomposites special properties.

Hydrobiotite is a vermiculite–phlogopite interstratified clay mineral, and it has a high charge density within the vermiculite interlayer spaces (Ran, 1998). Thereby, it is also possible that hydrobiotite can be intercalated with surfactant cations to prepare a novel type of surfactant–clay mineral complexes. Because of the existence of phlogopite layers, which has similar structures as montmorillonite/vermiculite but does not have any exchangeable cations, the obtained complexes may also have quite unique structural characteristics comparing with the complexes obtained from montmorillonite and vermiculite. In this work, cetyltrimethylammonium ($CTMA^+$) was selected as representative of cationic surfactant to intercalate hydrobiotite, and the structural evolution of the surfactant–hydrobiotite complexes were investigated increasing $CTMA^+$ loading. Structural properties of the complexes were derived from X-ray diffraction (XRD), Fourier transform infrared spectroscopy (FTIR) and thermogravity analysis (TG). Surfactant–montmorillonite complexes were also prepared for comparison. Results of this work may contribute to the preparation of novel surfactant–clay mineral complexes with unique structures and properties and understanding the intercalation mechanism of surfactants in clay minerals.

2. Materials and methods

2.1. Materials

Montmorillonite and hydrobiotite were obtained from Inner-Mongolia (China) and Xinjiang (China), respectively. The structural formula of montmorillonite and hydrobiotite are $Na_{0.02}K_{0.02}Ca_{0.39}[Fe_{0.45}Mg_{1.10}Al_{2.51}][Si_{7.91}Al_{0.09}]O_{20}(OH)_4{\cdot}nH_2O$ and $Na_{0.25}K_{0.45}Ca_{0.04}$ $[Fe_{0.58}Mg_{5.04}Al_{0.02}Ti_{0.12}]{\cdot}[Si_{5.84}Al_{2.16}]O_{20}(OH)_4{\cdot}nH_2O$ respectively (Zhu et al., 2007; Ran, 1998). Montmorillonite has a cation exchange capacity (CEC) value of 1.08 meq/g (i.e., charge density of 0.41 eq/mol), which is calculated directly from the structural formula. The charge sites on montmorillonite are mainly arising from the substitution of Al ion by Mg ion in the octahedron sheet, and each exchangeable charge site occupies an interlayer surface area (equivalent area A_{Mont}) of about 0.57 nm^2. Because a great part of the K^+ cations on hydrobiotite cannot be exchanged, the CEC value of hydrobiotite cannot be directly calculated from the structural formula. Thereby, the NH_4^+ exchange method was used to determine the CEC value of hydrobiotite, and the obtained value is 0.87 meq/g (i.e., charge density of 0.33 eq/mol). As the cations (K^+) in phlogopite interlayer spaces are non-exchangeable, CEC of hydrobiotite mainly contributes from vermiculite interlayer spaces, and each exchangeable charge site occupies an interlayer surface area (A_{Hyd}) of about 0.35 nm^2. It also shows that the negative charge on hydrobiotite mainly arises from the substitution of Si by Al in the tetrahedral sheets. Cetyltrimethylammonium bromide (CTMAB) was of analytical grade and obtained from Shanghai Chemical Co., China. Structure of CTMAB was shown in Fig. 1.

2.2. Preparation of surfactant–clay mineral complexes

Surfactant–clay mineral complexes were prepared as follows: 5.0 g of montmorillonite or hydrobiotite were dispersed in 100 mL of distilled water, and then desired amounts of CTMAB in amounts from 0.22 to 2.16 mmol/g and from 0.11 to 2.0 mmol/g were added for montmorillonite and hydrobiotite, respectively. The suspensions were stirred at 50 °C for 10 h, and then aged at 25 °C for one week. Subsequently, the products were washed by filtration for several times and dried at 80 °C for 8 h. The complexes synthesized from montmorillonite and hydrobiotite were designated as CTMA–Mont and CTMA–Hyd, respectively. CTMA–Mont complexes with different surfactant loading amounts were denoted as *x*C–Mont (*x* mean surfactant loading amount). For example, 21C–Mont represented the CTMA–Mont sample with the surfactant loading amount equal to 0.21 mmol/g, and the same notation was used for CTMA–Hyd complexes. All of the samples were grinded to pass 100 meshes and than characterized soon after drying.

2.3. Characterization

Organic-carbon contents (TOC) of the samples were analyzed with a SHIMADZU TOC-V CPH organic-carbon analyzer, and the adsorbed surfactant amounts were calculated according to the measured organic-carbon contents values. If the surfactant loading amounts were below the CEC, they were expected to be adsorbed as cations; if the surfactant loading amounts were above the CEC, they were expected to be adsorbed as both cations and molecules (surfactant in ion pairs). The clay mineral contents of the complexes were calculated by subtracting the surfactant contents from the complexes. The original montmorillonites and hydrobiotite without surfactant had organic-carbon content less than 0.04%. The XRD patterns were recorded using a Rigaku D/max-2550PC diffractometer with Cu Kα radiation. The samples were pressed in glass sample holders, and the range between 1° and 20° (2θ) was recorded with a scanning speed of 2°/min. FTIR spectra were recorded in the 4000–400 cm^{-1} region on a Thermo Nicolet Nexus 670 FTIR spectrophotometer, operating at a resolution of 1.0 cm^{-1}. Proper amount of samples and KBr were mixed together and milled to fine powder using a mortar

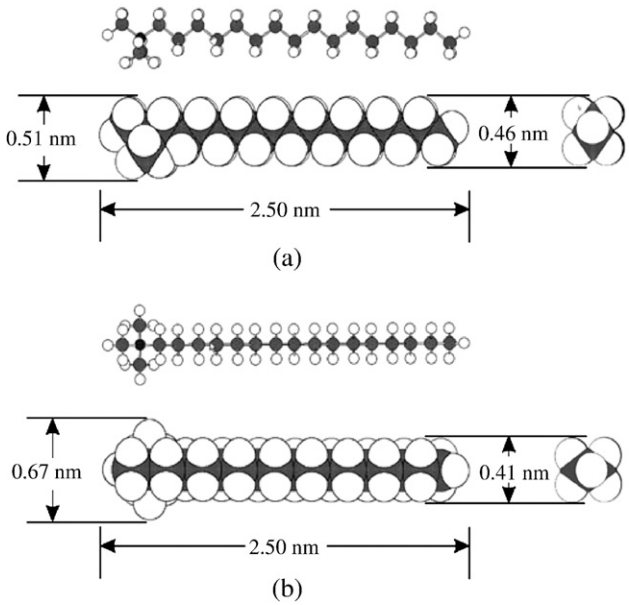

Fig. 1. Structure and dimensions of CTMAB.

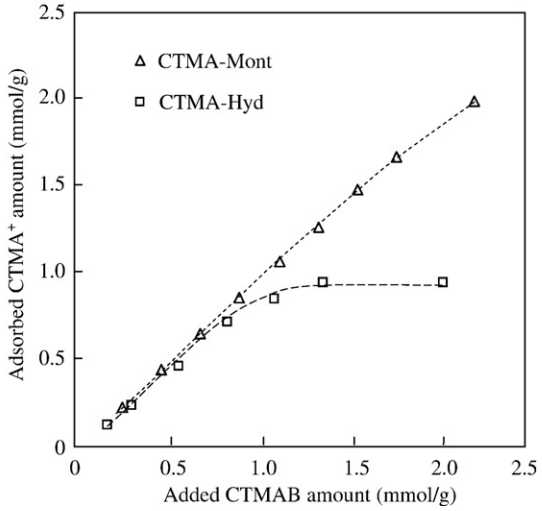

Fig. 2. Adsorption of $CTMA^+$ on montmorillonite and hydrobiotite.

and pestle. The powders were then made into a fragile pellet using a compression machine, and placed inside the pellet cell for analysis. Sixty four interferograms were collected for each sample. TG analysis was conducted on a TA instrument SDTQ600 under an air atmosphere. The samples were heated from room temperature to 750 °C at a rate of 10 °C/min. Derivative themogravimetric (DTG) curves were analyzed by derivative weight loss. The relative humidity of the air was in the range of 60–70% during the TOC, XRD and TG measurement process; while in the FTIR measurement process the relative humidity is controlled at around 55%.

3. Results and discussion

3.1. Surfactant loading amounts on montmorillonite and hydrobiotite

Fig. 2 presents the adsorbed surfactant amounts on the surfactant–clay mineral complexes. In the region of small added surfactant amounts (e.g.,<0.8 mmol/g), most of the added surfactants were adsorbed to the clay minerals. Montmorillonite adsorbed most of the surfactant (~1.98 mmol/g, or 1.83 CEC) even when the added surfactant reached 2.16 mmol/g (2.0 CEC). Hydrobiotite reached its maximum adsorption capacity (~0.93 mmol/g, or 1.06 CEC) at around 1.30 mmol/g of added surfactant. The difference of surfactant adsorption on the clay minerals can be ascribed to the difference of charge density of the clay minerals. Because of the higher charge density, each charge site on hydrobiotite will occupy less siloxane surface than on montmorillonite (A_{Mont}:A_{Hyd}=0.57:0.35). The head group of $CTMA^+$ covers a surface area of about 0.34 nm^2 (0.51 nm × 0.67 nm), just somewhat smaller than A_{Hyd} (0.35 nm^2) whereas much smaller than A_{Mont} (0.57 nm^2). Thereby, hydrobiotite can only adsorb surfactant amount a little larger than its CEC, whereas montmorillonite still can effectively adsorb surfactant even when the loading amount approached 2.0 CEC.

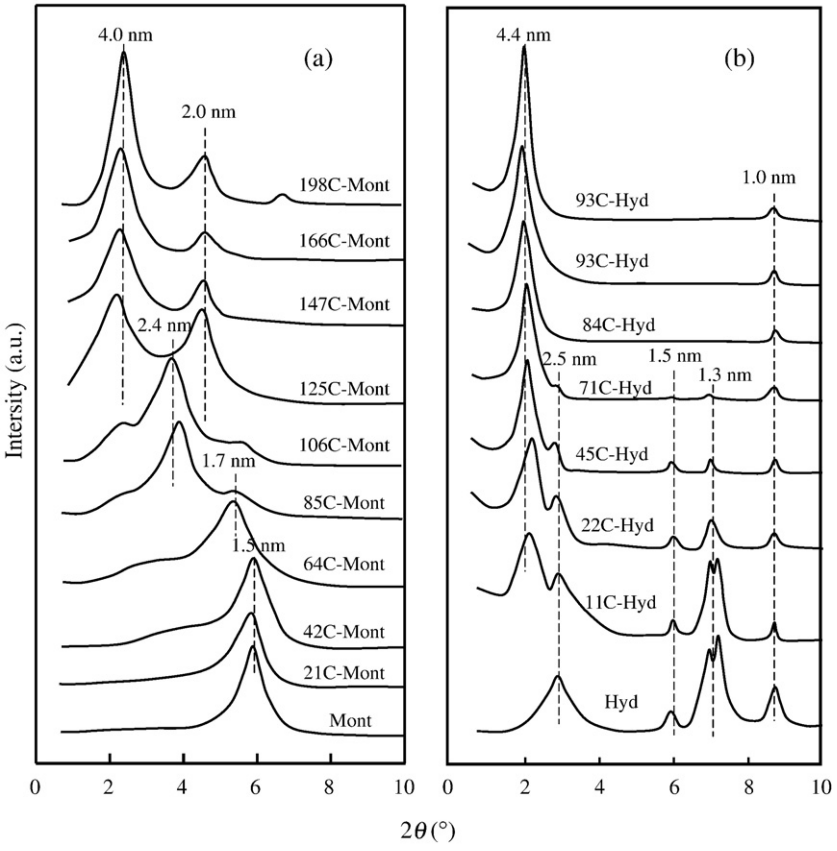

Fig. 3. XRD diagrams of CTMA–Mont (a) and CTMA–Hyd (b).

3.2. XRD characterization

XRD is known to be a useful method for characterizing structure of surfactant–clay mineral complexes (Zhu et al., 2003a,b; Lagaly and Dekany, 2005). Combined with the basal spacing values and dimensions of the surfactant molecule, arrangement models of the intercalated surfactants can be proposed (Weiss, 1963; Zhu et al., 2003a,b; Lagaly et al., 1975; Lagaly and Dekany, 2005; Bergaya et al., 2006). Fig. 3 presents the XRD patterns for CTMA–Mont (a) and CTMA–Hyd (b). Increasing surfactant loading amount led to a stepwise increase of d_{001} values of CTMA–Mont, which is in agreement with other reports (Zhu et al., 2003a,b; Chen et al., 2005). According to the reported surfactant arrangement models in previous investigations (Lagaly et al., 1975; Lagaly and Dekany, 2005; Bergaya et al., 2006; Zhu et al., 2003a,b; Chen et al., 2005), the lateral-monolayer (~1.5 nm), lateral-bilayer (~1.7 nm), pseudo-trilayer (~2.0 nm), paraffin-monolayer (~2.4 nm) and paraffin-bilayer (~4.0 nm) arrangement models could be proposed for the adsorbed surfactants within the montmorillonite interlayer spaces.

In respect to CTMA–Hyd, the XRD results were rather unique. With increasing surfactant loading amount, the d_{001} values of CTMA–Hyd increased to and then remained around 4.4 nm. The adsorbed surfactants were expected to adopt the paraffin-monolayer structure (4.4 − 1.0 = 3.4 nm). The reflections at around 2.5, 1.5 and 1.3 nm are the reflection of hydrobiotite, vermiculite and the (002) reflection of hydrobiotite, respectively (Ran, 1998). The intensity of these peaks gradually decreased with increasing surfactant loading and eventually disappeared. This implied that, with increasing surfactant loading amount, the interlayer spaces of hydrobiotite were expanded layer by layer rather than simultaneously. The peak at around 1.0 nm, corresponding to the diffraction of phlogopite, remained for all of the complexes, which indicated that the surfactant could not intercalate into the interlayer spaces of phlogopite.

3.3. FTIR characterization

FTIR has been widely used to probe the conformation of the adsorbed surfactant cations on clay minerals (Kung and Hayes, 1993; Vaia et al., 1994; Zhu et al., 2005). The CH_2 infrared absorption bands are sensitive to the ordering (or *gauche*/*trans* conformer ratio) and packing density of the surfactants, and interactions between the alkyl chains (Kung and Hayes, 1993; Vaia et al., 1994). The selected spectral regions between 3100 and 2700 cm^{-1} for CTMA–Mont and CTMA–Hyd were shown in Fig. 4. With increasing surfactant loading, both CH_2 asymmetric stretching modes ($\nu_{as}(CH_2)$) and symmetric stretching modes ($\nu_s(CH_2)$) of the adsorbed surfactant on CTMA–Mont gradually shifted to low frequency, until close to those of CTMAB solid (~2918 and 2850 cm^{-1}, respectively), which

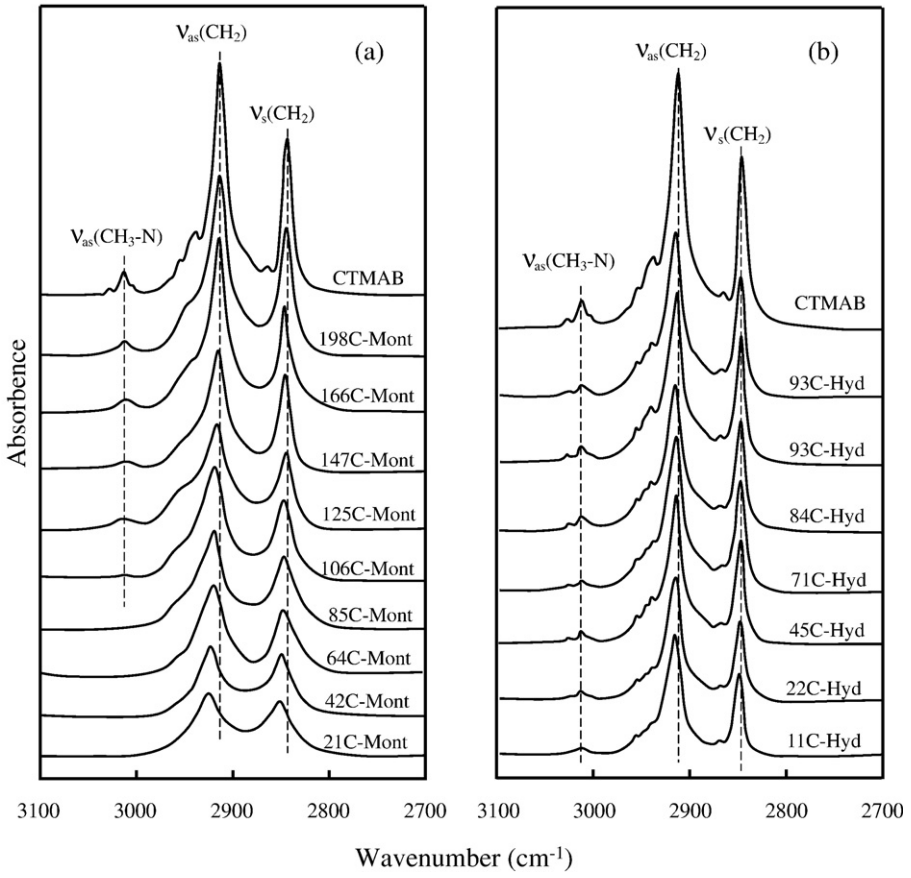

Fig. 4. FTIR patterns of CTMA–Mont (a) and CTMA–Hyd (b) in the region 3100–2700 cm^{-1}.

indicated that conformation of the adsorbed surfactants developed progressively from liquidlike (i.e., low packing density and ordering) to solidlike (i.e., high low packing density and ordering) (Vaia et al., 1994; Zhu et al., 2005). Increasing surfactant packing density will further lead to the expansion of clay mineral interlayer spaces, in agreement with the XRD characterization results.

In the case of CTMA–Hyd, the frequencies of both ν_{as} (CH_2) and ν_s(CH_2) modes were close to those of CTMAB solid even at very low surfactant loading level (e.g., 0.11 mmol/g), and the frequencies of these modes only show slight shift (less than 1 cm^{-1}) in the whole surfactant loading range. Absorption band at 3017 cm^{-1} for the CTMAB solid arises from the asymmetric stretching modes of the headgroup CH_3–N (ν_{as}(CH_3–N)) (Kung and Hayes, 1993), which appeared on CTMA–Mont only when the surfactant loading amount exceeded 1.25 mmol/g (i.e., 1.16 CEC), whereas it was observable for all CTMA–Hyd complexes. Above results indicated that the adsorbed surfactant on CTMA–Hyd had a conformation quite similar to solid CTMAB, i.e., high packing density and ordering. The relatively constant surfactant packing density was also the reason why all CTMA–Hyd complexes had similar d_{001} values.

3.4. TG characterization

Thermal analysis has been used for exploring the structures of surfactant–clay mineral complexes, as thermal characteristics of the adsorbed surfactants correlate well with their conformations (Li and Ishida, 2003; He et al., 2005; Hedley et al., 2007). The DTG curves of the CTMA–Mont (a) and CTMA–Hyd (b) (Fig. 5) show two peaks between 35–750 °C for CTMA–Mont. The peak at 63–93 °C corresponds to the loss of adsorbed water (He et al., 2005). With increasing surfactant loading, the peak shift gradually to low temperature range, as the environments become more hydrophobic as the surfactants loading increased (He et al., 2005; Xi et al., 2005a,b). The broad peak at 300–400 °C for 21C–Mont corresponds to loss of adsorbed surfactant. With increasing surfactant loading, the peak gradually shifted toward low temperature range until it was close to that of solid CTMAB (270 °C vs. 254 °C), and the shape of the peak gradually evolved from broad to sharp. This indicated that

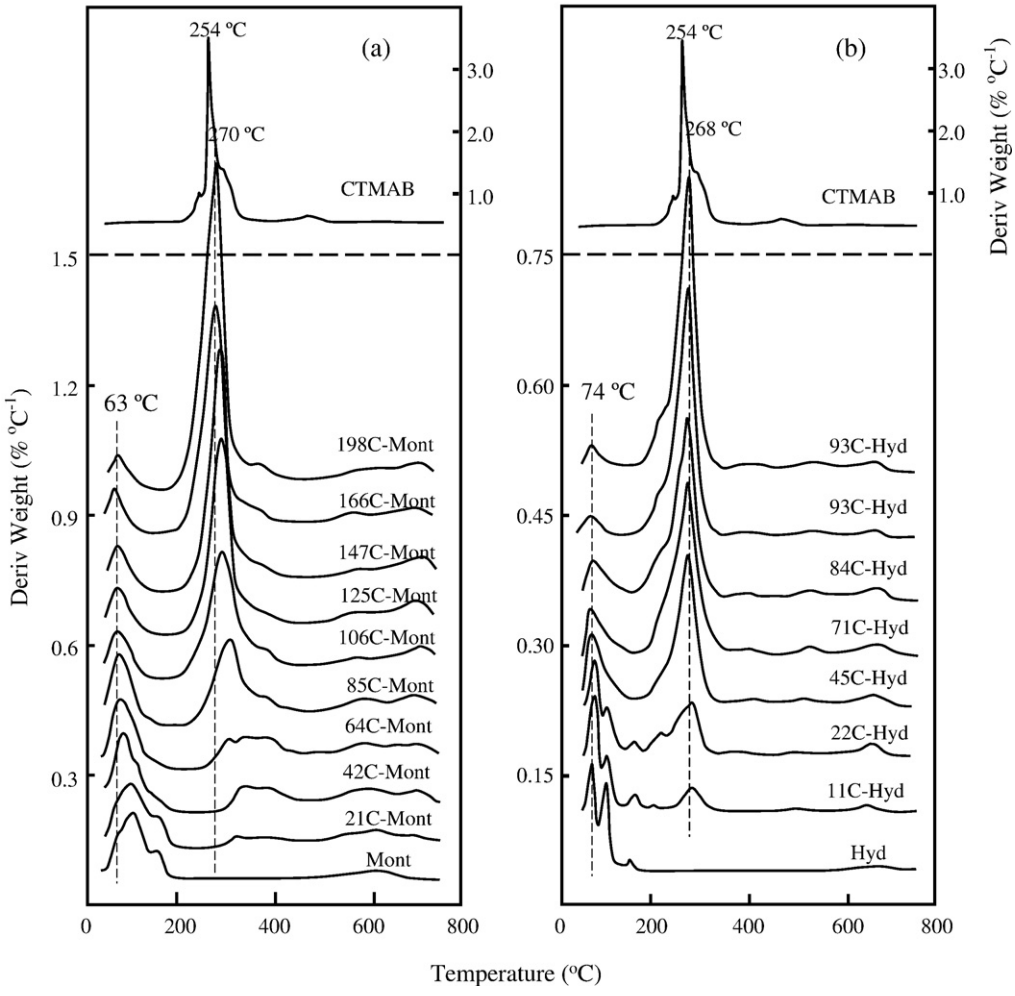

Fig. 5. Derivative thermogravimetric (DTG) curves of CTMAB solid, CTMA–Mont (a) and CTMA–Hyd (b).

conformations of the adsorbed surfactants were significantly influenced by the interlayer environment (e.g., hydrated inorganic cations) at low surfactant loading (He et al., 2005; Chen et al., 2005), and they were shown to resemble that of solid CTMAB at high surfactant loading, in agreement with the FTIR characterization.

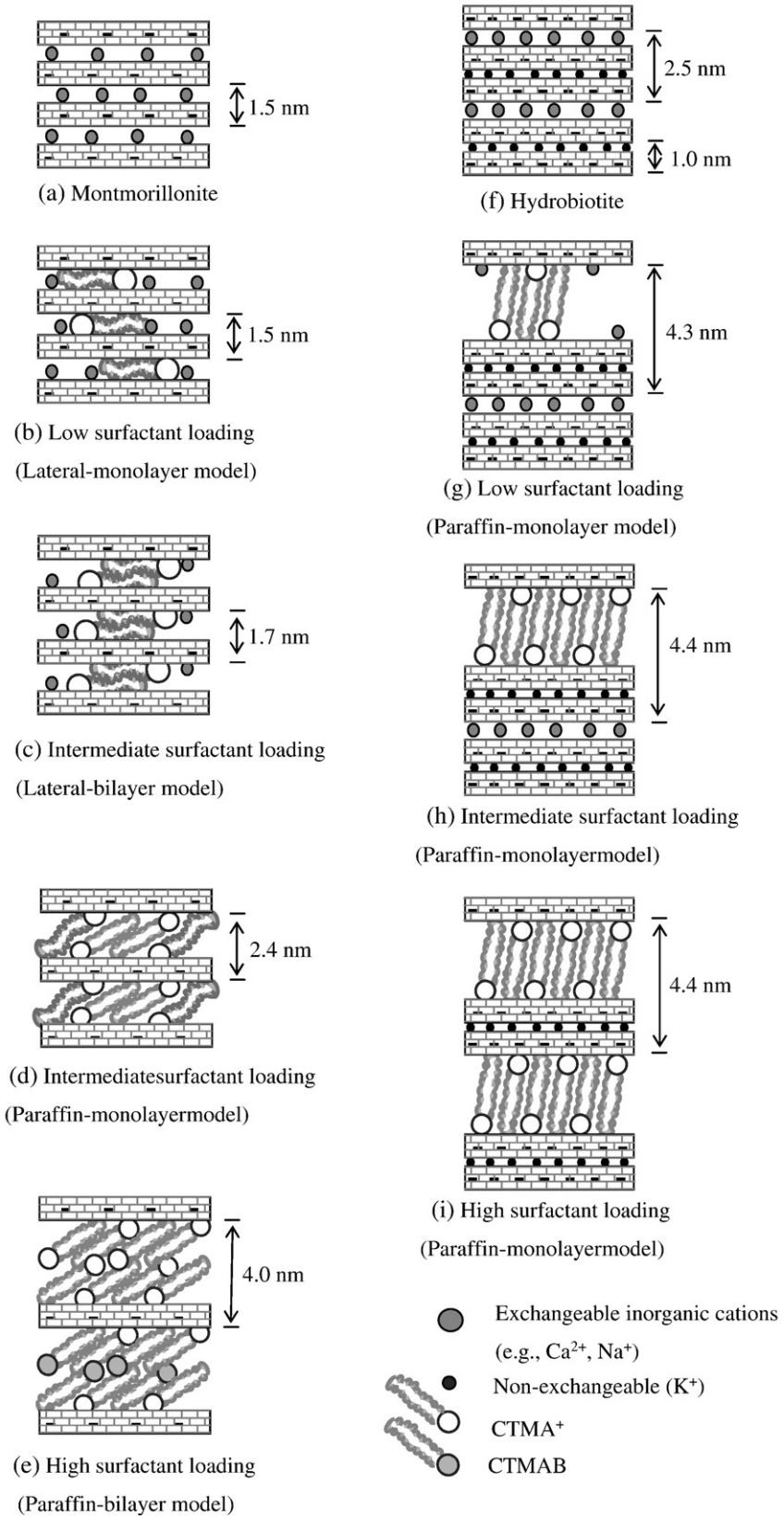

Fig. 6. Schematic drawing of the structural models of CTMA–Mont (b–e) and CTMA–Hyd (g–i).

In respect to CTMA–Hyd, the peaks corresponding to the losses of water and surfactants were not significantly changed in the whole surfactant loading range. The peaks corresponding to the losses of surfactants for CTMA–Hyd were close to that of the solid CTMAB (~268 °C vs. 254 °C). This indicated that even at low surfactant loading, the adsorbed surfactants did not interact strongly with the hydrated inorganic cations and had conformations similar to the solid surfactant. The peaks corresponding to the loss of water for CTMA–Hyd were close to that of the original hydrobiotite, which also indicated that there was no significant interaction between the adsorbed surfactants and the hydrated inorganic cations, in agreement with the FTIR characterization results.

3.5. Structural models of the surfactant–clay mineral complexes

Adsorption of surfactant on the clay mineral is basically a layer charge controlled "self-assembling" process (Heinz et al., 2003; Osman et al., 2004). Driving forces for surfactant intercalation include the electric interaction between positively charged surfactant head groups and the negative clay mineral charges and van der Waals interactions between the surfactant alkyl chains (Xu and Boyd, 1995; Osman et al., 2004). The structural difference of CTMA–Bent and CTMA–Hyd can be ascribed to their different charge characteristics.

Montmorillonite has relatively low charge density and the negative charges result from substitutions and defects in the octahedral sheet, which are weaker than in case of tetrahedral substitutions; thus the inorganic cations can be easily replaced by $CTMA^+$. Thereby, the van der Waals interaction seems to be less important in determining the location of the surfactant cations, and the surfactant cations are relatively free to replace the inorganic cations at different domains and layers. Thus, the adsorbed surfactants will form small surfactant patches rather than bulk surfactant aggregates at low surfactant loading level (Lee and Kim, 2002; Heinz et al., 2003). With increasing surfactant loading, the size of the small surfactant patches will grow and ultimately connect with each other to form large surfactant aggregates. Only then will most of the adsorbed surfactants interact directly with each other and adopt solidlike conformation.

Hydrobiotite has high charge density and the charge sites locate mainly on the tetrahedral sheets. Thereby, electric interaction between inorganic cations and charge sites is stronger and the inorganic cations on hydrobiotite cannot so easily be replaced by $CTMA^+$. Thus, both electric interaction and hydrophobic interaction will contribute to adsorption of surfactant cations on hydrobiotite, and $CTMA^+$ will prefer the charge sites adjacent to the pre-adsorbed $CTMA^+$ because of the additional hydrophobic interaction there. Subsequently, the surfactant cations will replace the inorganic cations on hydrobiotite layer by layer. Thereby, the adsorbed surfactant can form bulk surfactant aggregates even at very low surfactant loading level, and most of the intercalated surfactant cations will be surrounded by other surfactant cations rather than by inorganic cations. Moreover, as the available surface on hydrobiotite is rather small for each surfactant cation (0.35 nm^2 vs. 0.34 nm^2), the adsorbed surfactants have to pack closely; thus they have solidlike conformation over a wide loading range.

The proposed structural evolution processes for $CTMA^+$ intercalated montmorillonite and hydrobiotite are in well agreement with the characterization results. According to these analyses, the probable structures of the surfactant–clay mineral complexes were depicted in Fig. 6. Because of the unique structural characteristics of the CTMA–Hyd, they can find special utilities in different fields, for example, the adsorbed surfactants can be alternative for some lipid bilayers and soil organic matter with high packing densities.

4. Conclusions

Because of the difference of charge characteristics of the clay mineral, the $CTMA^+$ cations have quite different intercalation processes on hydrobiotite and montmorillonite. The inorganic cations on montmorillonite can be easily exchanged by $CTMA^+$; thus $CTMA^+$ can freely diffuse to the different charge sites on montmorillonite. Thereby, the interlayer spaces of montmorillonite can be expanded simultaneously, and conformations of the adsorbed surfactants are shown to develop progressively from liquidlike to solidlike with increasing surfactant loading. However, the inorganic cations on hydrobiotite cannot be exchanged so easily, and the surfactant cations will prefer the charge sites next to the pre-adsorbed surfactant cations. Thereby, the intercalated surfactant cations will form closely packed bulk phases on hydrobiotite and adopt solidlike conformation even at very low loading level, and interlayer spaces of hydrobiotite are expanded layer by layer.

Acknowledgements

This work was supported by grants from the National Natural Science Foundation of China (50378081).

References

Bergaya, F., Theng, B.K.G., Lagaly, G., 2006. Handbook of clay science, vol. 1. Elsevier, Amsterdam, pp. 309–378. Chap. 7.3.

Chen, B., Zhu, L., Zhu, J., Xing, B., 2005. Configurations of the bentonite-sorbed myristy-lpyridinium cation and their influences on the uptake of organic compounds. Environ. Sci. Technol. 39, 6093–6100.

Chtourou, M., Frikha, M.H., Trabelsi, M., 2006. Modified smectitic Tunisian clays used in the formulation of high performance lubricating greases. Appl. Clay Sci. 32, 210–216.

He, H., Ding, Z., Zhu, J., Yuan, P., Xi, Y., Yang, D., Frost, R.L., 2005. Thermal characterization of surfactant-modified montmorillonites. Clays Clay Miner. 53, 287–293.

He, H., Frost, R.L., Bostrom, T., Yuan, P., Duong, L., Yang, D., Xi, Y., Kloprogge, J.T., 2006. Changes in the morphology of organoclays with HDTMA+ surfactant loading. Appl.Clay Sci. 31, 262–271.

Hedley, C.B., Yuan, G., Theng, B.K.G., 2007. Thermal analysis of montmorillonites modified with quaternary phosphonium and ammonium surfactants. Appl. Clay Sci. 35, 180–188.

Heinz, H., Castelijins, H.J., Suter, U.W., 2003. Structure and phase transitions of alkyl chains on mica. J. Am. Chem. Soc. 125, 9500–9510.

Kung, K.S., Hayes, K.F., 1993. Fourier transform infrared spectroscopic study of the adsorption of cetyltrimethylammonium bromide and cetylpyridinium chloride on silica. Langmuir 9, 163–167.

Lagaly, G., 1976. Kink-block and Gauche-block structures of biomolecular films. Angew. Chem. Int. Ed. Engl. 15, 575–586.

Lagaly, G., Dekany, I., 2005. Adsorption on hydrophobized surfaces: clusters and self-organization. Adv. Colloid Interface 114, 189–204.

Lagaly, G., Fitz, St., Weiss, A., 1975. Kink block structures in clay organic complexes. Clays Clay Miner. 23, 45–54.

LeBaron, P.C., Wang, Z., Pinnavaia, T.J., 1999. Polymer-layered silicate nanocomposites: an overview. Appl. Clay Sci. 15, 11–29.

Lee, S.Y., Kim, S.J., 2002. Expansion characteristics of organoclay as a precursor to nanocomposites. Coll. Surf. A 21, 19–26.

Li, Y., Ishida, H., 2003. Concentration-dependent conformation of alkyl tail in the nanoconfined space: hexadecylamine in the silicate galleries. Langmuir 19, 2479–2484.

Lin, J.J., Cheng, I.J., Wang, R., Lee, R.J., 2001. Tailoring basal spacings of montmorillonite by poly(oxyalkylene) diamines intercalation. Macromolecules 34, 8832–8834.

Murray, H.H., 2000. Traditional and new applications for kaolin, smectite and polygorskite: a general overview. Appl. Clay Sci. 17, 207–221.

Osman, M.A., Ploetze, M., Skrabal, P., 2004. Structure and properties of alkylammonium monolayers self-assembled on montmorillonite platelets. J. Phys. Chem. B. 108, 2580–2588.

Osman, M.A., 2006. Organo-vermiculites: synthesis, structure and properties. Platelike nanoparticles with high aspect ratio. J. Mater. Chem. 16, 3007–3013.

Ran, H., 1998. The interstratified structure and interlayer nature of hydrobiotite in Weili. Ph.D Dissertation. Guangzhou Institute of Geochemistry, Academia Sinica.

Vaia, R.A., Teukolsky, R.K., Giannelis, E.P., 1994. Interlayer structure and molecular environment of alkylammonium layered silicates. Chem. Mater. 6, 1017–1022.

Venkatatraman, N.V., Vasudevan, S., 2003. Cholesterol binding to the alkyl chains of an intercalated surfactant bilayer. J. Phys. Chem. B 107, 10119–10126.

Weiss, A., 1963. Organic derivatives of mica-type layer-silicates. Angew. Chem. Int. Ed. 2, 134–144.

Witthuhn, B., Klauth, P., Klumpp, E., Narres, H.D., Martinius, H., 2005. Sorption and biodegradation of 2,4-dichlorophenol in the presence of organoclays. Appl. Clay Sci. 28, 55–66.

Xi, Y., Frost, R.L., He, H., Kloprogge, T., Bostrom, T., 2005a. Modification of Wyoming montmorillonite surfaces using a cationic surfactant. Langumir 21, 8675–8680.

Xi, Y., Martens, W., He, H., Frost, R.L., 2005b. Thermogravimetric analysis of organoclays intercalated with the surfactant octadecyltrimethylammonium bromide. J. Therma. Anal. Cal. 81, 91–97.

Xu, S., Boyd, S.A., 1995. Cationic surfactant adsorption by swelling and nonswelling layer silicates. Langmuir 11, 2508–2514.

Yariv, S., 2002. Organo-clay complexes and interactions. Marcel Dekker. Inc., New York.

Zhu, J., He, H., Guo, J., Yang, D., Xie, X., 2003a. Arrangement models of alkylammonium cations in the interlayer of $HDTMA^+$ pillared montmorillonites. Chin. Sci. Bull. 48, 368–372.

Zhu, L., Chen, B., Tao, S., Chiou, C.T., 2003b. Interactions of organic contaminants with mineral-adsorbed surfactants. Environ. Sci. Technol. 37, 4001–4006.

Zhu, J., He, H., Zhu, L., Wen, X., Deng, F., 2005. Characterization of organic phases in the interlayer of montmorillonite using FTIR and ^{13}C NMR. J. Colloid Interface Sci. 286, 239–244.

Zhu, L., Ren, X., Yu, S., 1998. Use of cetyltrimethylammonium bromide-bentonite to remove organic contaminants of varying polar character from water. Environ. Sci. Technol. 32, 3374–3378.

Zhu, R., Zhu, L., Xu, L., 2007. Sorption characteristics of CTMA–bentonite complexes as controlled by surfactant packing density. Coll. Surf. A 294, 221–227.